

## Brief Reports

# Striatal Gray Matter Loss in Huntington's Disease Is Leftward Biased

Mark Mühlau, MD,<sup>1\*</sup> Christian Gaser, PhD,<sup>2</sup>  
Afra M. Wohlschläger, PhD,<sup>1,3,4</sup> Adolf Weindl, MD,<sup>1</sup>  
Michael Städtler,<sup>1</sup> Michael Valet, MD,<sup>1</sup>  
Claus Zimmer, MD,<sup>3</sup> Jan Kassubek, MD,<sup>5</sup>  
and Alexander Peinemann, MD<sup>1</sup>

<sup>1</sup>Department of Neurology, Technische Universität München, Munich, Germany; <sup>2</sup>Department of Psychiatry, University of Jena, Jena, Germany; <sup>3</sup>Department of Neuroradiology and <sup>4</sup>Department of Nuclear Medicine, Technische Universität München, Munich, Germany; <sup>5</sup>Department of Neurology, University of Ulm, Ulm, Germany

**Abstract:** In Huntington's disease (HD), the distribution of pathological changes throughout the brain is incompletely understood. Some studies have identified leftward-biased lateralization, whereas others did not. We performed magnetic resonance imaging and a voxel-based asymmetry analysis in 44 right-handed HD gene carriers (presymptomatic, n = 5; stage I, n = 28; stage II, n = 11) and 44 right-handed healthy controls. The group comparison revealed leftward-biased gray matter loss in the striatum. Further analyses showed no indication of asymmetry in presymptomatic HD patients but an increase in asymmetry in the course of the HD stages under examination. Our study demonstrates and discusses leftward-biased gray matter loss in HD. © 2007 Movement Disorder Society

**Key words:** gray matter loss; Huntington's disease; lateralization, striatum; voxel-based morphometry

Huntington's disease (HD) is an autosomal dominant neurodegenerative disease. Since the discovery that HD results from an expanded CAG trinucleotide,<sup>1</sup> HD has become an attractive model for the study of neurodegeneration. However, the pathomechanisms that lead to the typical distribution of pathological changes throughout

the brain (i.e., neuronal loss and astrocytosis primarily in the striatum) and the clinical picture of HD are poorly understood. The development of animal models has led to numerous discoveries related to the mutant gene product huntingtin; however, far from arriving at a unifying mechanism, robust evidence suggests that multiple — probably interacting — pathomechanisms occur in HD. Therefore, a comprehensive model of HD must account for multiple pathomechanisms and interactions and, in this way, explain the distribution of pathological changes throughout the brain. However, data on this distribution are conflicting, even with respect to the basic question of lateralization.<sup>2,3</sup> Addressing this issue, we performed a whole-brain asymmetry analysis in HD based on voxel-based morphometry (VBM).

VBM enables the detection of subtle structural changes throughout the brain at group level using magnetic resonance imaging (MRI). The main idea of VBM asymmetry analysis comprises the following steps: (1) spatial normalization of all images to a symmetric anatomical space to allow averaging; (2) segmentation of images into gray matter (GM), white matter (WM), as well as cerebrospinal fluid (CSF); (3) calculation of difference images using the lateralization index; and (4) group comparison of GM asymmetry across the whole brain.

## SUBJECTS AND METHODS

### Subjects

Data and images were derived from routine diagnostics of our HD outpatient clinic that participates in the European Huntington Disease Network (<http://www.euro-hd.net/html/network>) and from healthy volunteers who had participated in other imaging studies at our department. The HD group (women, 23) consisted of 44 gene-positive right-handed subjects (lateralization index, >70%).<sup>4</sup> Five patients were presymptomatic (Motor score of the Unified HD Rating Scale [mUHDRS], 0; Mini-Mental State Examination, > 26). There were 28 patients who were in stage I and 11 who were in stage II according to Shoulson and Fahn.<sup>5</sup> Further details on the HD group are given in Table 1.

Healthy controls were matched for age (within 2 yr) and sex in a pair-wise manner (right-handers, 44;

\*Correspondence to: Dr. Mark Mühlau, Technische Universität München, Department of Neurology, Möhlstrasse 28, D-81675 München, Germany. E-mail: m.muehlau@neuro.med.tum.de

Received 2 March 2006; Revised 26 June 2006; Accepted 26 June 2006

Published online 29 March 2007 in Wiley InterScience (www.interscience.wiley.com). DOI: 10.1002/mds.21137

**TABLE 1.** Characterization of the HD patients

	Min.	Max.	Median	Mean	SD
Age <sup>a</sup>	24	68	42	45	11
Onset age <sup>b</sup>	24	62	40	42	10
Time since onset	0	14	4.0	4.4	3.7
MMSE	18	30	28	27	3.1
mUHDRS <sup>a</sup>	0	62	13	18	17
CAG <sup>c</sup>	40	49	43	44	2.4

<sup>a</sup>Age correlated significantly with mUHDRS (Spearman correlation coefficient, 0.74; two-sided  $P$  value, <0.001).

<sup>b</sup>Onset was defined as the occurrence of first motor symptoms.

<sup>c</sup>CAG repeats correlated significantly with onset age (Spearman correlation coefficient, -0.52; two-sided  $P$  value, 0.002).

CAG, number of CAG trinucleotide repeats; Max., maximum; Min., minimum; MMSE, Mini-Mental State Examination;<sup>15</sup> mUHDRS, Motor score of the Unified Huntington's Disease Rating Scale.<sup>12</sup>

women, 23; mean age, 44 yr; standard deviation of age, 9.1).

### Magnetic Resonance Imaging

Each participant underwent MRI in the same scanner (magnetic field intensity, 1.5 Tesla; scanner, *Siemens Magnetom Symphony*; sequence, T1 magnetization prepared rapid gradient echo (MPRAGE); plane, sagittal; number of slices, 160; slice thickness, 1 mm; voxel size,  $1 \times 1 \times 1$  mm<sup>3</sup>; flip angle, 15 degrees; field of view,  $256 \times 256$  mm). After 27 HD patients and their corresponding controls had undergone MRI (TR, 11.1 msec; TE, 4.3 msec; TI, 800 msec), *Siemens* performed a software upgrade by installing the "*syngo software*," which resulted in slightly different parameters of the standard MPRAGE sequence (TR, 8.9 msec; TE, 3.93 msec; TI, 800 msec). To certainly exclude an effect of this software upgrade, the sequence was included in each analysis as confounding covariate (see below). SPM2 software (Wellcome Department of Imaging Neuroscience Group, London, UK; <http://www.fil.ion.ucl.ac.uk/spm>) was applied for data processing.

### Voxels Included in the Analyses

We included only voxels with a GM value greater than 0.2 (maximum value, 1) and greater than both the WM and CSF value to analyze only voxels with sufficient GM and to avoid possible edge effects around the border between GM, WM, and CSF. Accounting for possible misclassification of GM throughout the basal ganglia, we also included all voxels of the caudate and lentiform nucleus as defined with the Wake Forest University (WFU) -Pick Atlas.<sup>6</sup>

### "Conventional" Optimized VBM Analysis

At first, we performed "conventional" VBM according to the "optimized" protocol<sup>7</sup> using study-specific prior

probability maps, the modulation step, and a Gaussian kernel of 8 mm for smoothing. The values of the resulting images indicate the voxel-wise probability of GM and are commonly interpreted as absolute GM.<sup>7</sup> Voxel-by-voxel analysis of covariance (ANCOVA) was used to detect absolute GM differences between both groups. In this analysis, age, sex, total GM volume (derived from the first segmentation process), and MPRAGE sequence of each participant were included as confounding covariates. Using the family wise error,<sup>8</sup> we applied a height threshold of  $P < 0.05$  corrected for multiple comparisons at the voxel level and an extent threshold of  $P < 0.05$  corrected at the cluster level. The areas identified by the "conventional" VBM analysis were used as a region of interest (ROI) for the asymmetry analysis.

### Asymmetry Analysis

The asymmetry analysis is an extension of VBM and has been validated and described in detail elsewhere.<sup>9</sup> In accordance with this analysis, we used a study-specific symmetric template and study-specific symmetric probability maps for GM, WM, and CSF. Otherwise, the preprocessing steps were identical to the "conventional" optimized VBM analysis described above. In an additional step before smoothing, we generated a new set of GM images by calculating a difference image (DI) for each participant. For this purpose, the original GM images (origGM) were flipped along the midsagittal plane (flipGM). Then, we calculated the lateralization index of each voxel by applying the following formula:  $DI = (\text{origGM} - \text{flipGM}) / (0.5 [\text{origGM} + \text{flipGM}])$ .

To compare the brain asymmetry of HD patients with that of healthy controls, we used the smoothed DIs of all 88 participants for ANCOVA (ROI, voxels identified by the "conventional" VBM analysis; height threshold,  $P < 0.05$  corrected; extent threshold,  $P < 0.05$  corrected).<sup>8</sup> Because GM decreases with age in healthy subjects, age should be included as a confounding covariate in "conventional" VBM analyses.<sup>7</sup> Because motor impairment significantly correlated with age (Spearman coefficient, 0.74; two-sided  $P$  value, < 0.001) in our sample of patients, we, at first, tested the necessity to include age as confounding covariate in our asymmetry analysis. For this purpose, we performed a regression analysis of asymmetry with age in the control group. As we did not find age-related asymmetry, we included only sex and MPRAGE sequence but not age as confounding covariates in the asymmetry analysis. The applied contrast *Controls > HD* indicates areas that, in HD, contain less GM compared to the corresponding areas of the other hemisphere while also controlling for the asymmetry of both the control group and MRI sequence.

Finally, we analyzed asymmetry with regard to increase in the course of the disease and performed a multiple regression analysis (with constant) of GM asymmetry with motor impairment as determined with mUHDRS (ROI, voxels identified by the asymmetry analysis; height threshold, 0.05 corrected; extent threshold, 0.05 corrected; additional regressors, sex and MPRAGE sequence). To examine whether lateralization already exists at the presymptomatic stage or emerges in the course of the disease, we used the volume of interest function of SPM2 and extracted the raw values of the cluster showing significant correlation with motor impairment from both the HD and control group. The values of the HD group were then plotted against the mUHDRS and compared to the 5th and 95th percentile of the control group.

## RESULTS

In accordance with previous studies,<sup>2,10,11</sup> the “conventional” VBM analysis (Fig. 1A; Table 2) demonstrated GM loss in the HD group that was most prominent in the striatum. Furthermore, regions with GM loss were identified in the frontal, parietal, and occipital lobe (Table 2). The asymmetry analysis (Fig. 1B) showed highly significant leftward-biased striatal GM loss in HD patients. Peak voxels were located in the putamen and in the head of the caudate nucleus (coordinates according to the Montreal Neurological Institute [MNI],  $-16, 11, -1$  and  $-8, 10, 6$ ; Z values, 6.9 and 6.6). Within the predefined ROI of GM asymmetry, regression analysis of GM asymmetry with motor impairment revealed the left putamen (MNI coordinates of peak voxel,  $-20, 5, -2$ ; Z value, 3.9; Fig. 1C, left panels). The raw values of the cluster derived from both the HD and control group are shown in Figure 2. Without masking, regression analysis of GM asymmetry with motor impairment yielded a cluster that is also localized in the putamen (MNI coordinates of peak voxel,  $-16, 11, -1$ ; Z value, 6.9) but posteriorly extends outside the ROI (Fig. 1C, right panels).

## DISCUSSION

In the present study, lateralization of pathological changes in HD throughout the whole brain was analyzed on a statistical basis. As we had no a priori hypothesis for asymmetries of areas apart from those displaying GM decrease (in HD compared to healthy controls), we first performed a “conventional” optimized VBM analysis (Fig. 1A) to derive a ROI for the asymmetry analysis. This asymmetry analysis revealed highly significant leftward-biased GM decrease in the striatum (Fig. 1B). In a further analysis, we investigated whether asymmetry of

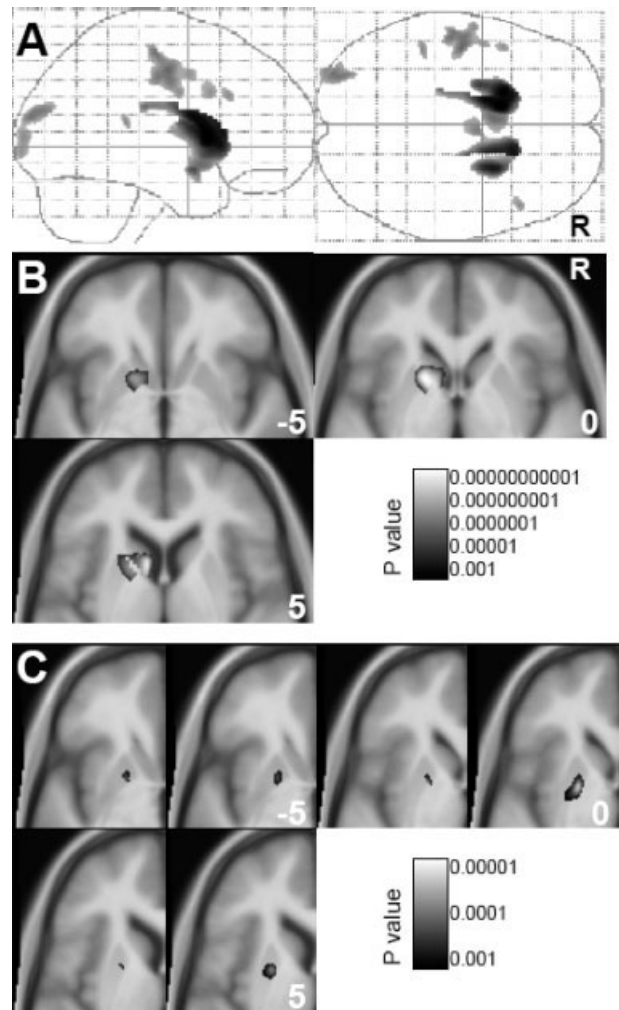


**FIG. 1.** Gray matter loss and its asymmetry in Huntington's disease. **A:** Shown are maximum intensity projections of gray matter (GM) decrease throughout the whole brain (height threshold,  $P < 0.05$  corrected; extent threshold,  $P < 0.05$  corrected; “conventional” voxel-based morphometry analysis). The right side of the images is indicated with “R”. **B:** Gray matter asymmetry is projected onto axial slices of the study-specific averaged T1-image (region of interest [ROI], GM decrease as shown in A; height threshold,  $P < 0.05$  corrected; extent threshold,  $P < 0.05$  corrected). As indicated by the bar on the lower right, increasing significance is coded from black to white. According to the Montreal Neurological Institute standard brain, coordinates (z axis) of axial slices are indicated in the right lower corner of each slice. **C:** Correlation of GM asymmetry with the Motor score of the Unified Huntington's Disease Rating Scale is projected onto axial slices. Significant voxels of the predefined ROI (i.e., GM asymmetry as shown in B) are shown in the left panel of each slice, whereas the whole cluster that posteriorly extends outside the ROI is shown in the respective right panels.

striatal GM loss changes in the course of the disease. For this purpose, we performed a regression analysis of asymmetry with motor impairment in the HD group. Again, we performed a ROI analysis because we had no a priori hypothesis for areas apart from that displaying

**TABLE 2.** Areas of gray matter decrease in Huntington's disease

Cluster size in voxels (1 × 1 × 1 mm)	MNI coordinates x, y, z	Z values of peak voxels	Area
10842	-11, 10, 7	<7.5	L caudate body
	-18, 12, 6	7.8	L putamen
	-15, 16, 6	7.6	L caudate head
	-17, 18, 2	7.6	L caudate head
	-24, -1, 14	6.9	L putamen
	-16, 6, 10	6.4	L putamen
	-14, 6, 6	6.1	L putamen
	-21, -25, 24	6.0	L caudate body
	-19, -18, 25	5.8	L caudate body
	6608	15, 19, 10	7.5
25, 7, 8		7.4	R putamen
16, 5, 20		7.2	R caudate body
18, -8, 25		6.4	R caudate body
24, 13, -3		6.2	R putamen
19, 6, 14		4.8	R putamen
11, 19, 1		4.7	R caudate head
2997	-48, -11, 46	6.1	L frontal lobe, precentral g., BA4
	-53, -18, 56	5.9	L parietal lobe, postcentral g., BA3
	-55, -17, 41	5.8	L frontal lobe, postcentral g., BA4
1475	-30, -90, 18	5.9	L occ. lobe, middle occ. g., BA19
	-29, -83, 22	5.7	L occ. lobe, superior occ. g., BA19
	-31, -94, 5	5.4	L occ. lobe, middle occ. g., BA19
197	-44, -35, 14	5.4	L temp. lobe, superior temp. g., BA29
203	48, 23, 30	5.4	R frontal lobe, middle frontal g., BA46
239	-46, 13, 32	5.3	L frontal lobe, middle frontal g., BA9

MNI, Montreal Neurological Institute; BA, Brodmann area; g., gyrus; L, left; occ., occipital; R, right; temp., temporal.

GM asymmetry. In this way, leftward-biased GM loss was shown to significantly increase with motor impairment. In accordance with the primary role of the putamen in motor function, the respective cluster extended outside the ROI toward more posterior areas of the putamen (Fig. 1C). The comparison of the asymmetry values (derived from the cluster correlating with motor impairment) between the HD and control group (Fig. 2) indicated that leftward-biased striatal GM asymmetry is not present in

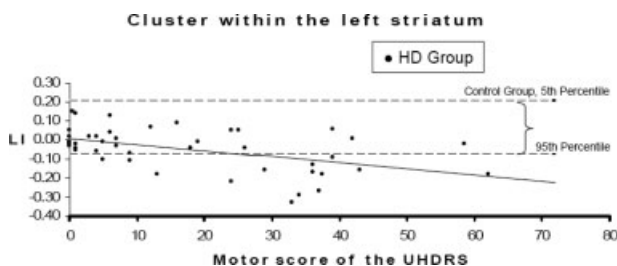


**FIG. 2.** Correlation of striatal asymmetry and motor impairment in Huntington's disease (HD). Asymmetry values (lateralization index, LI) of the HD group are plotted (black dots) against the motor score of the Unified Huntington's Disease Rating Scale (UHDRS; Spearman correlation coefficient,  $-0.45$ ; two-sided  $P$  value,  $0.002$ ). For comparison, the 5th and 95th percentile of the respective values from the control group are indicated with dashed lines. Values were derived from the cluster (within the predefined region of interest) identified by the regression analysis of gray matter asymmetry with motor impairment.

presymptomatic HD but occurs with the development of symptoms.

So far, the only study reporting leftward-biased lateralization of pathological changes in HD on a statistical basis used MR spectroscopy. Jenkins and colleagues described a "curious" leftward-biased increase in lactate levels in the striatum. By the use of VBM, Thieben and associates<sup>2</sup> found GM decrease in the striatum bilaterally but this GM decrease showed "unexpected" asymmetry reaching only borderline significance on the right, whereas no particular analysis was performed to verify this leftward lateralization. In contrast, Kassubek and coworkers did not report leftward lateralization of GM loss but did not perform an asymmetry analysis either.<sup>11</sup>

The present study confirms the assumption that, in HD, pathological changes of the striatum are biased to the left (i.e., to the dominant hemisphere). This leftward biased GM asymmetry seems not to exist in presymptomatic stages of HD but to occur with symptoms (Fig. 2). Popular pathomechanisms that have been related to HD such as glutamatergic excitotoxicity<sup>13</sup> and mitochondrial dysfunction,<sup>14</sup> by nature, increase with neuronal activity. Therefore, we suggest that a surplus of cumulative life time activity in the left compared to the right striatum causes leftward-biased striatal GM loss in HD as also proposed by Jenkins and colleagues<sup>3</sup> and Thieben

and associates.<sup>2</sup> Such an asymmetry of overall striatal activity is well conceivable. All patients included in this study were right-handed; handedness displays the clearest example of behavioral lateralization, goes along with a more frequent use of the dominant hand and, hence, results in higher activity of cortical and subcortical motor areas of the dominant hemisphere. In future studies, left-handed HD patients should be investigated in pre-symptomatic and symptomatic stages to address the influence of handedness.

In summary, we evaluated the asymmetry of GM loss in HD and found leftward lateralization in the striatum. We propose that, primarily compatible with the pathomechanisms of excitotoxicity, a surplus of cumulative synaptic activity in the dominant striatum causes this leftward-biased GM loss.

## REFERENCES

1. The Huntington's Disease Collaborative Research Group. A novel gene containing a trinucleotide repeat that is expanded and unstable on Huntington's disease chromosomes. *Cell* 1993;72:971–983.
2. Thieben MJ, Duggins AJ, Good CD, et al. The distribution of structural neuropathology in pre-clinical Huntington's disease. *Brain* 2002;125:1815–1828.
3. Jenkins BG, Rosas HD, Chen YC, et al. 1H NMR spectroscopy studies of Huntington's disease: correlations with CAG repeat numbers. *Neurology* 1998;50:1357–1365.
4. Oldfield RC. The assessment and analysis of handedness: the Edinburgh inventory. *Neuropsychologia* 1971;9:97–113.
5. Shoulson I, Fahn S. Huntington disease: clinical care and evaluation. *Neurology* 1979;29:1–3.
6. Maldjian JA, Laurienti PJ, Kraft RA, Burdette JH. An automated method for neuroanatomic and cytoarchitectonic atlas-based interrogation of fMRI data sets. *Neuroimage* 2003;19:1233–1239.
7. Good CD, Johnsrude IS, Ashburner J, Henson RN, Friston KJ, Frackowiak RS. A voxel-based morphometric study of ageing in 465 normal adult human brains. *Neuroimage* 2001;14:21–36.
8. Friston KJ, Holmes A, Poline JB, Price CJ, Frith CD. Detecting activations in PET and fMRI: levels of inference and power. *Neuroimage* 1996;4:223–235.
9. Luders E, Gaser C, Jancke L, Schlaug G. A voxel-based approach to gray matter asymmetries. *Neuroimage* 2004;22:656–664.
10. Rosas HD, Koroshetz WJ, Chen YI, et al. Evidence for more widespread cerebral pathology in early HD: an MRI-based morphometric analysis. *Neurology* 2003;60:1615–1620.
11. Kassubek J, Juengling FD, Kioschies T, et al. Topography of cerebral atrophy in early Huntington's disease: a voxel based morphometric MRI study. *J Neurol Neurosurg Psychiatry* 2004; 75:213–220.
12. Huntington Study Group. Unified Huntington's Disease Rating Scale: reliability and consistency. *Mov Disord* 1996;11:136–142.
13. DiFiglia M. Excitotoxic injury of the neostriatum: a model for Huntington's disease. *Trends Neurosci* 1990;13:286–289.
14. Schapira AH. Mitochondrial function in Huntington's disease: clues for pathogenesis and prospects for treatment. *Ann Neurol* 1997;41:141–142.
15. Folstein MF, Folstein SE, McHugh PR. "Mini-mental state". A practical method for grading the cognitive state of patients for the clinician. *J Psychiatr Res* 1975;12:189–198.

## Myoclonus–Dystonia Syndrome With Severe Depression Is Caused by an Exon-Skipping Mutation in the $\epsilon$ -Sarcoglycan Gene

Anjum Misbahuddin, MRCP,<sup>1</sup> Mark Placzek, BSc,<sup>1</sup> Graham Lennox, FRCP,<sup>2</sup> Jan-Willem Taanman,<sup>1</sup> and Thomas T. Warner, FRCP<sup>1\*</sup>

<sup>1</sup>Department of Clinical Neurosciences, Royal Free and University College Medical School, London, United Kingdom; <sup>2</sup>Department of Neurology, Addenbrookes Hospital, Cambridge, United Kingdom

**Abstract:** We describe two affected individuals in a family with myoclonus–dystonia syndrome complicated with severe depression. One individual committed suicide. Molecular genetic analysis revealed a heterozygous point mutation in the  $\epsilon$ -sarcoglycan gene, which we show leads to skipping of exon 5. This report suggests that the psychiatric spectrum of MDS includes more severe depression. © 2007 Movement Disorder Society

**Key words:** myoclonus–dystonia syndrome; depression;  $\epsilon$ -sarcoglycan mutation; exon skipping

Myoclonus–dystonia syndrome (MDS; OMIM 159900) is an autosomal dominant condition characterized by myoclonic jerks affecting the upper body and focal or segmental dystonia (e.g., cervical dystonia, writer's cramp).<sup>1</sup> Myoclonus affects proximal more than distal muscles and can be action-induced. Symptoms are often ameliorated by alcohol. There is also an association with obsessive–compulsive disorder, anxiety, and panic attacks.<sup>1–3</sup> These features are felt to be primary manifestations of the disease. Alcohol and benzodiazepine abuse is seen and thought to be secondary to use in alleviating symptoms.

This autosomal dominant disorder is caused by heterozygous mutations in the  $\epsilon$ -sarcoglycan gene (*SGCE*) on chromosome 7q21.<sup>4</sup> MDS is 30% to 40% penetrant with evidence of maternal imprinting,<sup>5</sup> and RT-PCR has revealed expression of only the paternal allele in lymphocytes in most cases studied.<sup>6</sup> Numerous different mutations have been described in exons 2 to 9 in *SGCE*<sup>4,7–10</sup> and usually result in a truncated protein either

\*Correspondence to: Dr. Thomas T. Warner, Department of Clinical Neurosciences, Royal Free and University College Medical School, Rowland Hill Street, London NW3 2PF, United Kingdom. E-mail: t.warner@medsch.ucl.ac.uk

Received 30 March 2006; Revised 9 September 2006; Accepted 10 September 2006

Published online 17 January 2007 in Wiley InterScience (www.interscience.wiley.com). DOI: 10.1002/mds.21297